University of Amsterdam

Assignment 3

EV Adoption, Coordination, and Policy Intervention

December 15, 2025

Students:
Noah Zuijderwijk
16493559

Māra Učelniece
14063549

Lecturer:
Mike Lees

Course:
Model-Based Decision Making

1 Introduction

The spread of a new technology across a social network depends on its structure and on agents' utility maximization. This report explores the transition to EVs using a networked agent-based model (ABM).

In our ABM, agents interact on the basis of a Stag Hunt game. This setup generates bistability: a high-adoption (cooperation) equilibrium where payoff is high, and a low-adoption (defection) equilibrium where conventional vehicles offer a steady but lower payoff. Crucially, the payoff for EV adoption is dynamically coupled to the level of EV infrastructure. As adoption increases, infrastructure improves, which further enhances the payoff for cooperation, creating a positive feedback loop.

We implement our ABM across three distinct model network topologies—Erdős–Rényi (ER) random networks, Watts–Strogatz (WS) small-world networks, and Barabási–Albert (BA) scale-free networks—to systematically examine how network topology influences adoption (Barabási & Albert, 1999; Erdős & Rényi, 1960; Watts & Strogatz, 1998). Through simulations on these model networks, we aim to identify emergent behaviors, like tipping and path dependence, that could provide model-based insights for policy interventions.

2 Methods

2.1 Model Specification

At each discrete time step, every agent i engages in a pairwise interaction with all its neighbors ($j \in N_i$), using its strategy ($S_i(t)$) of either C (Cooperation) or D (Defection). The payoff agent i receives from this Stag Hunt game against neighbor j is described by the following matrix ($a_I > b > 0$):

Table 1: Payoff Matrix for the EV Stag Hunt Game

Agent 1 \ Agent 2	**C**	**D**
C	(a_I, a_I)	$(0.0, b)$
D	$(b, 0.0)$	(b, b)

The total payoff ($P_i(t)$) for agent i:

$$P_i(t) = \sum_{j \in N_i} \text{Payoff}(S_i(t), S_j(t))$$

Additionally, payoff a_I increases with a global infrastructure variable $I(t)$ that is scaled by sensitivity parameter β_I:

$$a_I = a_0 + \beta_I I(t)$$

Infrastructure evolves globally as a function of current adoption $X(t)$:

$$I(t+1) = I(t) + g_I(X(t) - I(t))$$

At the end of each time step, agents update their strategy by applying an imitation rule. Each agent i compares its own total payoff ($P_i(t)$) with the total payoffs of all its neighbors ($P_j(t)$). Agent i then selects the strategy (C or D) that generated the maximum payoff in its immediate neighborhood, adopting it as its strategy for the next time step.

2.2 Experimental Design

We analyzed the networks' unforced dynamics by conducting parameter sweeps over the initial adoption X_0, initial infrastructure I_0, and infrastructure feedback strength β_I (Table 2). This allowed us to map the full (X_0,I_0) phase space to the mean final adoption X^*, identifying critical tipping thresholds and regions of path dependence. Then, we analyzed the effect of underlying network topology on adoption dynamics by exploring how adoption and infrastructure change over time in both baseline and intervention settings. We implemented three policy interventions: (1) targeted seeding by selecting for the highest-degree nodes (2) timed infrastructure shocks with random seeding (3) timed infrastructure shocks with highest-degree targeted seeding. These interventions test the relative efficacy of structural leverage (targeting high-degree nodes) versus temporal leverage (timing an infrastructure shock) in pushing the system towards tipping.

Table 2: Summary of Simulation Parameters

Category	Parameter (Symbol)	Value / Range	Description
Model Payoffs & Feedback			
	Baseline Payoff (a_0)	2.0	Payoff for two adopters when $I = 0$.
	Defection Payoff (b)	1.0	Payoff for defection when $I = 0$.
	Infrastructure Sensitivity (β_I)	2.0 (Baseline)	How much infrastructure I increases a_I.
	Infrastructure Update Rate (g_I)	0.05	Rate at which I adjusts toward adoption X.
Network Structure			
	Network Type ($-$)	ER, WS or BA	The type of underlying model network.
	Number of Nodes (N)	200	Total number of agents.
	New Edges per Step (m)	2	Edges added by a new node (for BA).
	Average Degree (k)	4	Degree of every node before rewiring (for WS)
	Edge Probability p	0.05	Edge formation (for ER) and rewiring (for WS)
Simulation Dynamics			
	Strategy Update Rule ($-$)	"imitate"	Agents copy neighbor with highest payoff.
	Total Time Steps (T)	200	Duration of each simulation run.
Experimental Setup (Heatmap)			
	X_0 Grid Points (X_0)	20 (from 0.0 to 1.0)	Initial adoption levels tested.
	I_0 Grid Points (I_0)	20 (from 0.0 to 1.0)	Initial infrastructure levels tested.
	Trials per Cell ($-$)	8	Monte Carlo trials per (X_0, I_0) cell.
	Seed (-)	42	
Experimental Setup (Phase Plots)			
	Trajectory Cases ((X_0, I_0))	6 pairs (e.g., $(0.40, 0.20)$	Starting points to illustrate dynamic paths.
	Seed (-)	42	
Experimental Setup (Sensitivity)			
	β_I Range (β_I)	20 points (from 0.0 to 4.0)	Infrastructure sensitivity values tested.
	X_0 Test Values (X_0)	4 values (0.2 to 0.5)	Fixed X_0 levels for sensitivity plot.
	Trials per Point ($-$)	8	Monte Carlo trials per (β_I, X) point.
	Seed (-)	42	
Experimental Setup (Policy Interventions)			
	Shock Times (t)	$25, 75, 125$	Shock times tested.
	Trials (T)	100	Monte Carlo trials per (t, X) and (t, I) point.

Parameters were chosen to experiment on the system's key dynamics, while maintaining computational efficiency. The Number of Nodes (N=200) and Total Time Steps (T=200) were chosen to observe emergent network phenomena while allowing for the Monte Carlo trials required for the heatmaps and sensitivity analysis. Additionally, the baseline payoffs ($a_0 = 2.0, b = 1.0$) configure the Stag Hunt coordination game with two stable outcomes. The small Infrastructure Update Rate ($g_I = 0.05$) ensures a slow co-evolution of adoption and infrastructure, necessary for observing dynamic paths.

3 Results

3.1 Baseline Analysis

Heatmaps and phase plots show that, depending on the model network, the system tips along a critical unstable boundary that separates defection equilibrium ($X^* \approx 0$) from the adoption equilibrium ($X^* \approx 1$) (Fig. 1). This separatrix is sharp and well-defined in the ER and WS networks, but becomes less sharp in the BA network (Fig. 1 a-c). Phase plots provide a local, temporal view, illustrating how the agents evolve to their final states. The trajectories confirm that the system quickly moves away from the separatrix, either moving to the defection equilibrium or toward the adoption equilibrium depending on the initial state (Fig. 1 d-f). The infrastructure feedback strength, governed by (β_I) has no distinguishable effect on any of the model networks (Fig. 2). The initial conditions (X_0,I_0) contribute more to system dynamics than the strength of the infrastructure feedback (within the tested range).

3.2 Structure Analysis

Phase plots (Fig. 1 d–f) show that the WS network exhibits slower adoption speeds compared to ER and BA networks. This, in combination with the adoption rates (Appendix Table 3), indicates that WS diffusion progresses locally but is delayed globally. This reflects strong cluster-level reinforcement but weaker inter-cluster coordination, which contrasts BA's hub-dependent stagnation or acceleration and ER's steady, uniform adoption.

The Monte Carlo simulation results (Appendix Table 3) indicate that WS networks have the highest frequency of reaching a high-adoption equilibrium across initial conditions, while BA networks have the lowest, despite BA's potential for rapid cascades. These observations coincide with a relatively much higher clustering coefficient for the WS network (0.444; Appendix Table 3) compared to the ER (0.046; Appendix Table 3) and BA (0.122; Appendix Table 3) networks. Additionally, the phase-space separatrix, sharp for ER and WS but diffuse for BA (Fig. 1), indicates that BA's degree heterogeneity increases variability near the tipping point.

3.3 Policy Intervention

The WS network exhibits the most policy-relevant behavior (Fig. 4). This network responds to targeted degree seeding of bridge nodes as well as infrastructure shocks (Fig. 4 c-d). Random degree seeding and highest-degree seeding without infrastructure shocks yield lower adoption than their counterparts with infrastructure shocks (Fig. 4). Simultaneously, highest-degree seeding always yields higher adoption than its random seeding counterpart regardless of infrastructure shocks (Fig. 4).

For the ER and BA networks, random seeding does not achieve the necessary positive feedback for reaching the cooperation equilibrium (Fig. 3 a-b & 4 a-b). However, targeting high-degree nodes kick-starts the system and pushes it beyond the tipping point (Fig. 3 c-d & 4 c-d). For the ER network, statistical outliers (high-degree nodes) help the system reach a critical mass of adoption. In the BA network, high-degree nodes form hubs that easily access the rest of the network and cause cooperation cascades. Targeted seeding for both then nearly voids the effect of infrastructure shocks (Fig. 3 e-f & 4 e-f), except for a slight effect of timed infrastructure shocks in the ER network where this drives remaining defecting nodes into cooperation (Fig. 3 g).

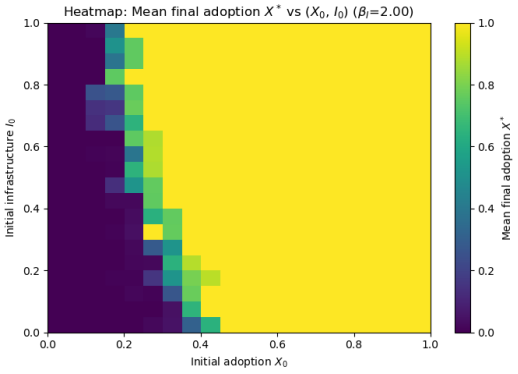

(a) Erdős–Rényi (ER)

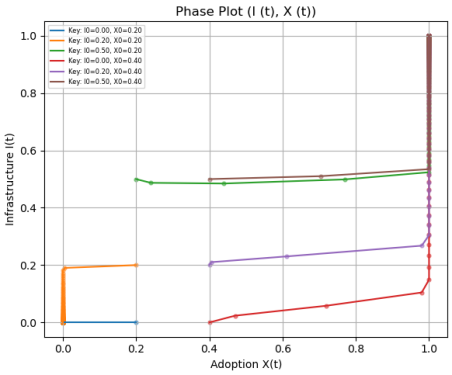

(d) Erdős–Rényi (ER)

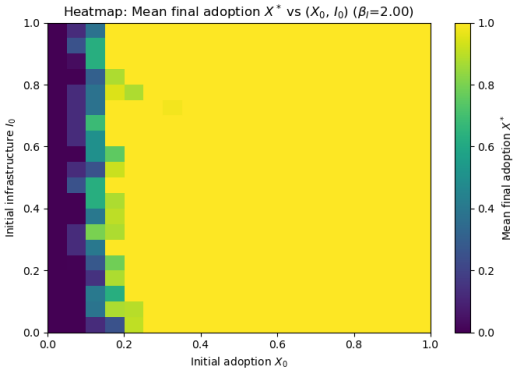

(b) Watts–Strogatz (WS)

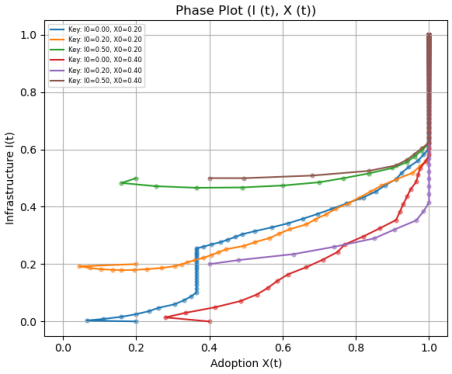

(e) Watts–Strogatz (WS)

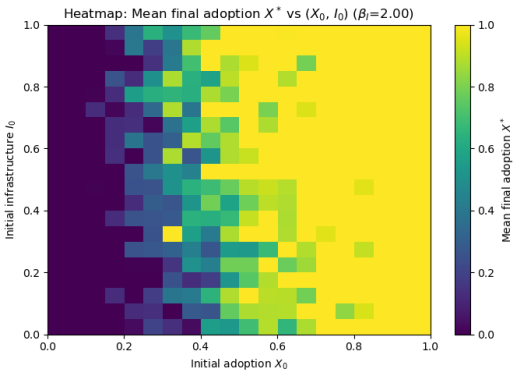

(c) Barabási–Albert (BA)

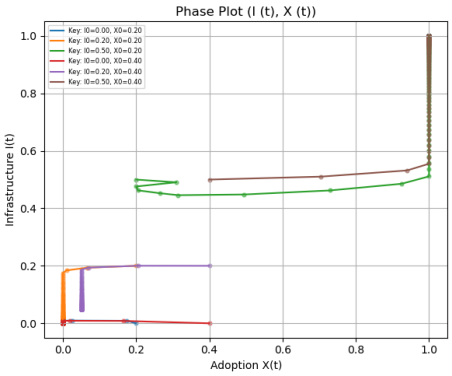

(f) Barabási–Albert (BA)

Figure 1: Tipping Behavior and Coupled Phase Dynamics of EV Adoption across Three Network Topologies ($\beta_I = 2.0$). Heatmaps show the mean final adoption (X^*) over the initial condition space (X_0 vs I_0) in the left column (a, b, c). Separatrixes form between the low-adoption (blue) and high-adoption (yellow). Phase Plots illustrate the path dependence (d, e, f). Each colored line is a single trajectory starting from a set initial condition, with markers indicating successive time steps.

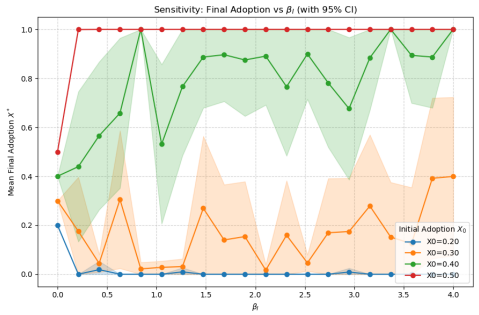

(a) Erdős–Rényi (ER)

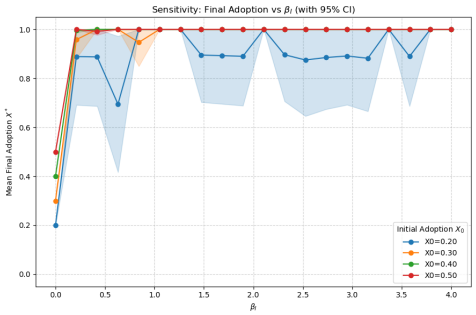

(b) Watts–Strogatz (WS)

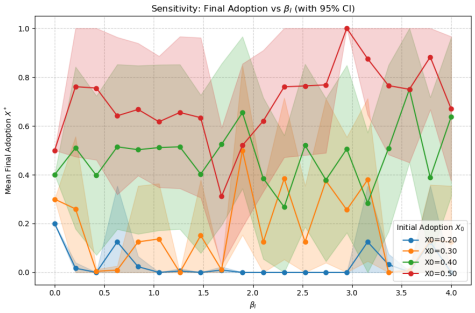

(c) Barabási–Albert (BA)

Figure 2: Sensitivity of Mean Final Adoption to Infrastructure Responsiveness (β_I) Across Model Network Types with 95% Confidence Intervals (N=8). Initial adoption values range from 0.20 to 0.50 with intervals of 0.10.

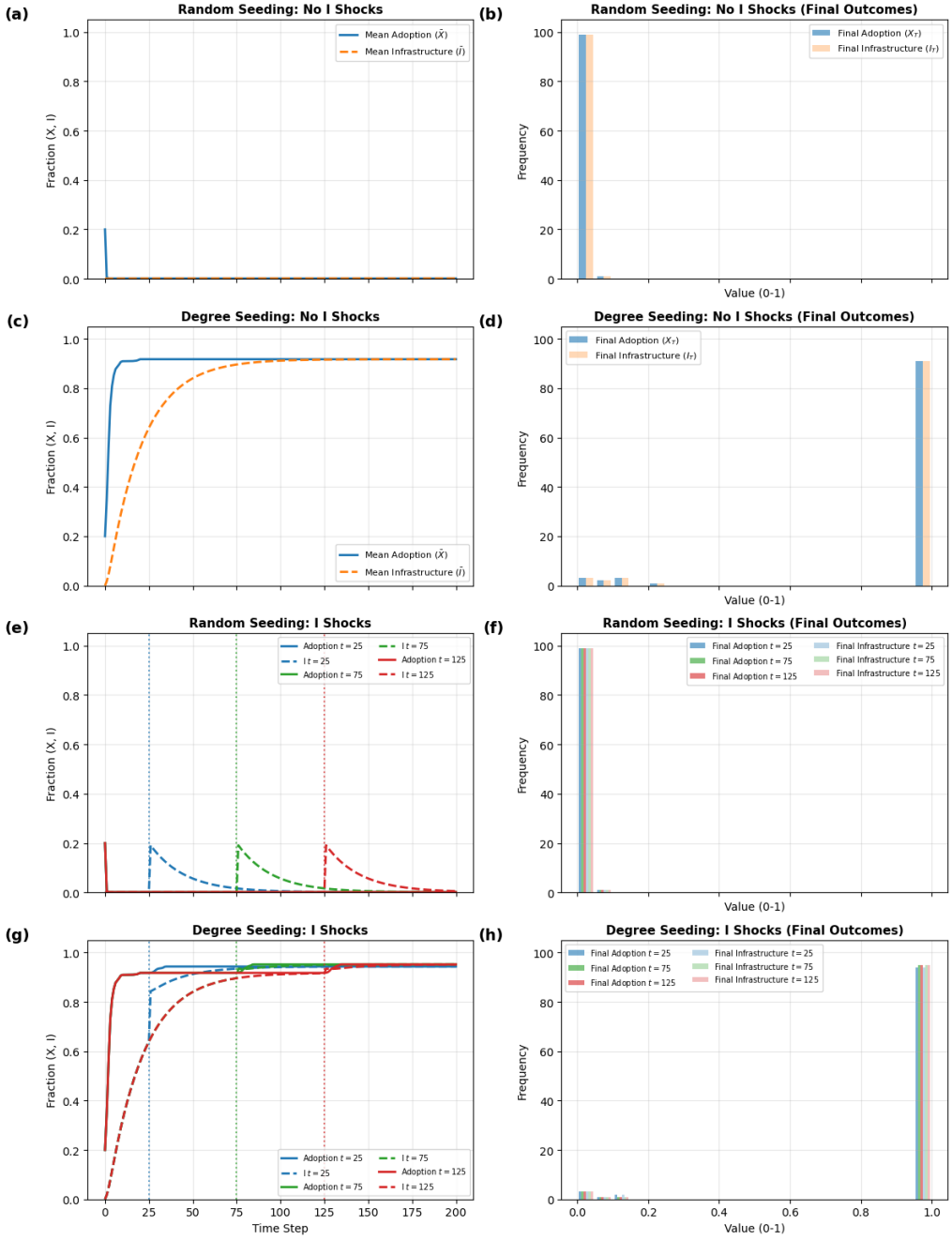

Figure 3: Intervention Effects on EV Adoption and Infrastructure in ER Network: Targeted seeding vs. Infrastructure Shocks. Left column contains plots with mean adoption and mean infrastructure over time, while right column displays the count of final outcomes for both variables. (a & b) present random seeding without infrastructure shocks (c & d) present highest-degree seeding without infrastructure shocks (e & f) present random seeding with infrastructure shocks, and (g & h) present highest-degree seeding with infrastructure shocks (N=100).

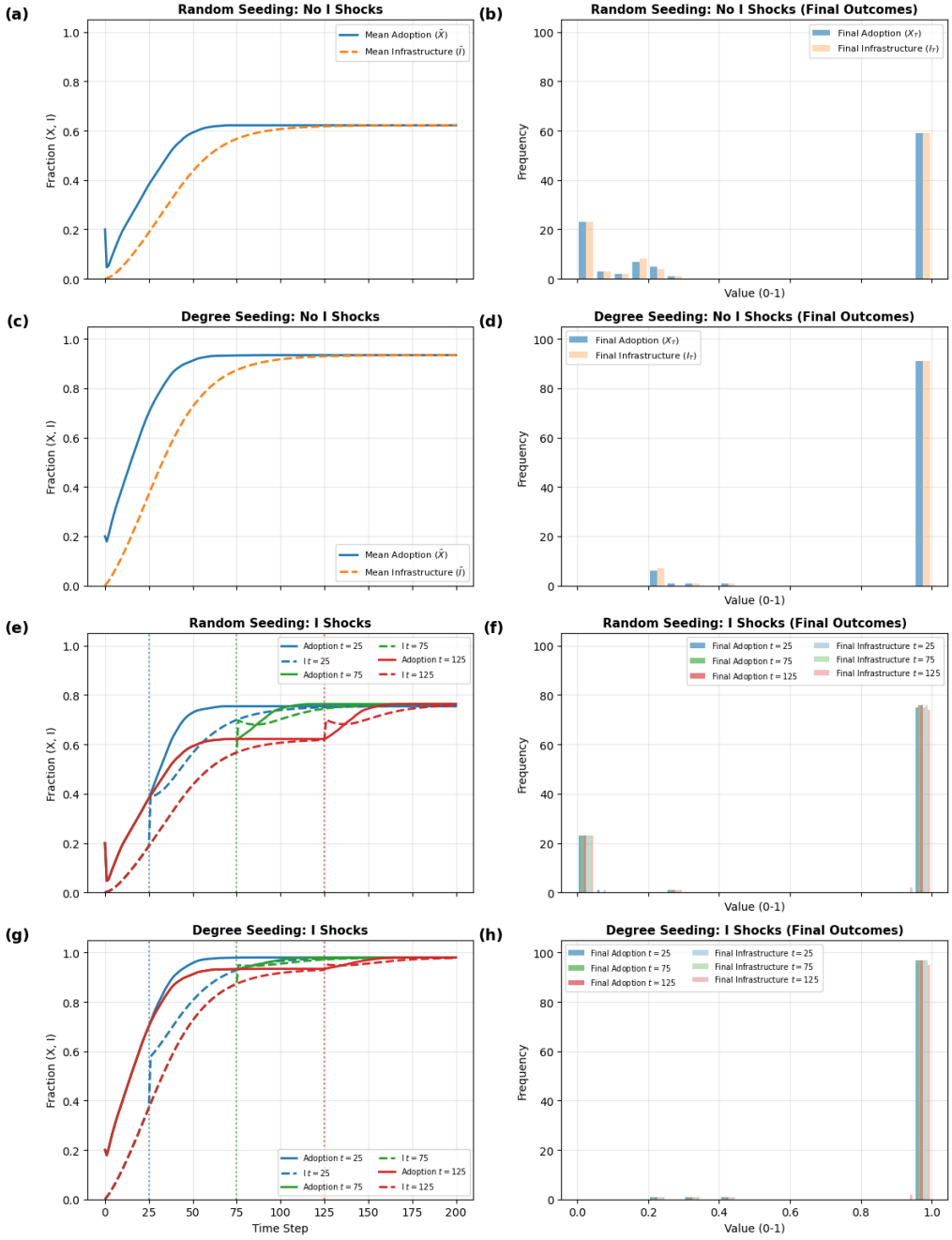

Figure 4: Intervention Effects on EV Adoption and Infrastructure in WS Network: Targeted seeding vs. Infrastructure Shocks. Left column contains plots with mean adoption and mean infrastructure over time, while right column displays the count of final outcomes for both variables. (a & b) present random seeding without infrastructure shocks (c & d) present highest-degree seeding without infrastructure shocks (e & f) present random seeding with infrastructure shocks, and (g & h) present highest-degree seeding with infrastructure shocks (N=100).

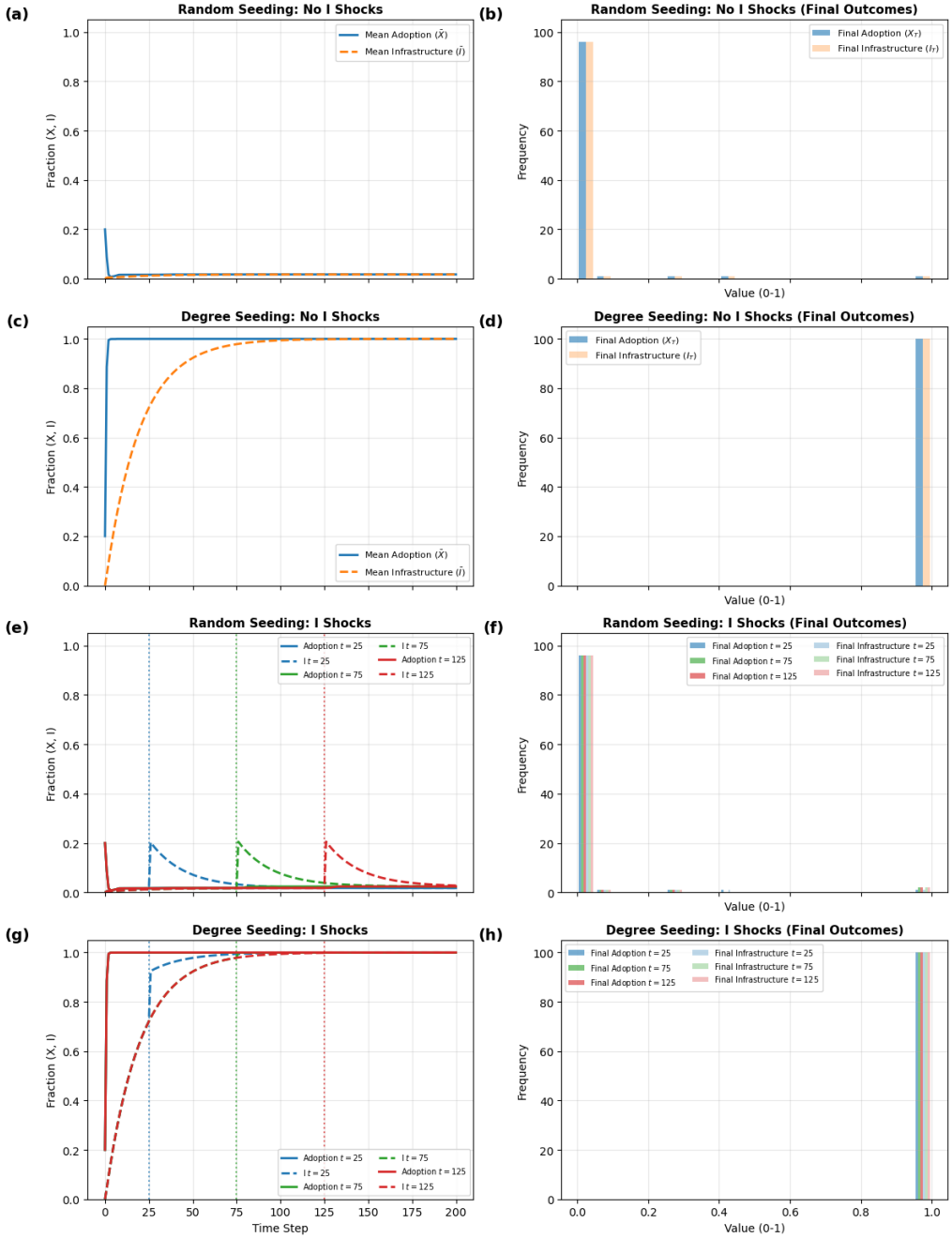

Figure 5: Intervention Effects on EV Adoption and Infrastructure in BA Network: Targeted seeding vs. Infrastructure Shocks. Left column contains plots with mean adoption and mean infrastructure over time, while right column displays the count of final outcomes for both variables. (a & b) present random seeding without infrastructure shocks (c & d) present highest-degree seeding without infrastructure shocks (e & f) present random seeding with infrastructure shocks, and (g & h) present highest-degree seeding with infrastructure shocks (N=100).

4 Discussion

In the EV transition model, the system displays emergent behavior. The positive infrastructure feedback combined with network structure is responsible for generating tipping points, path dependence, and bistability (Fig. 1). Small, early differences in initial conditions can push the system onto radically different trajectories, leading to two long-term outcomes: full system-wide cooperation or defection. These characteristic also make the system susceptible to targeted policy interventions.

In particular, the WS network has a fragile global coordination structure where policy effectiveness depends critically on where interventions are activated. This means the WS network is governed by structural leverage. The ER and BA networks experience quick adoption cascades when high-degree nodes are targeted due to their uniform degree distribution (ER) and hub-dominated structure (BA), respectively. This confirms that the ER and BA networks utilize high-degree nodes for rapid, network-wide dissemination, making structural leverage the most impactful policy for them as well.

4.1 Implications

This model's EV adoption dynamics can be applied to real-world social networks. Licciardi and Monteiro (2024) argue that networks of social contacts reflect small-world and scale-free elements. Therefore, results from WS and BA model networks contain some real-world relevance.

In scale-free (BA) social networks with preferential attachment and highly concentrated influence, the entire network can be accessed through key opinion leaders (hubs) regardless of when EV infrastructure is added. In contrast, small-world (WS) networks present a challenge due to high clustering, meaning the system's success hinges on bridging individuals, not singular hubs. For these networks, structural barriers necessitate a focus on policy targeting. For example, deployment of a public charging corridor (bridge node) at the moment global adoption begins to stagnate could overcome local cluster stability and drive system-wide coordination.

These differences underscore that successful EV transition requires a network-aware strategy that matches policy instruments to the specific topological characteristics of real-world networks.

4.2 Limitations

Conclusions from models cannot be blindly applied to real-world policy. The model networks are stylized and may not fully capture the complexity and multiplexity of real-world social networks. Besides, the limited number of Monte Carlo trials, time steps and the network sizes may have introduced stochastic uncertainty. Additionally, agent behavior is modeled using a single imitation-based strategy update rule. More rational behavioral rules may alter the system's tipping behavior. Also, infrastructure and adoption shocks are modeled exogenously and discretely, whereas real-world interventions are typically continuous and adaptive. Finally, the analysis focuses on static network structures, excluding co-evolutionary effects where agent adoption behavior might lead to changes in the network topology.

References

[Barabási and Albert(1999)] Barabási, A.-L., & Albert, R. (1999). Emergence of scaling in random networks. *Science*, 286(5439), 509–512. https://doi.org/10.1126/science.286.5439.509

[Erdős and Rényi(1960)] Erdős, P., & Rényi, A. (1960). On the evolution of random graphs. *Publications of the Mathematical Institute of the Hungarian Academy of Sciences*, 5. Retrieved from https://snap.stanford.edu/class/cs224w-readings/erdos60random.pdf

[Licciardi and Monteiro(2024)] Licciardi, N., & Monteiro, L. H. A. (2024). A Network Model of Social Contacts with Small-World and Scale-Free Features, Tunable Connectivity, and Geographic Restrictions. *Mathematical Biosciences & Engineering*, 21(4), 4801–4813. https://doi.org/10.3934/mbe.2024211

[Watts and Strogatz(1998)] Watts, D. J., & Strogatz, S. H. (1998). Collective dynamics of 'small-world' networks. *Nature*, 393(6684), 440–442. https://doi.org/10.1038/30918

5 Appendix

Network	X_0	I_0	Adoption Rate	Adoption Probability	Clustering Coefficient
ER	0.10	0.50	-0.0003	0.000	0.046
	0.30	0.50	0.0017	1.000	
	0.50	0.50	0.0013	1.000	
	0.50	0.00	0.0013	1.000	
	0.30	0.00	-0.0004	0.000	
	0.10	0.00	-0.0003	0.000	
	0.50	0.20	0.0013	1.000	
	0.30	0.20	0.0017	1.000	
	0.10	0.20	-0.0003	0.000	
WS	0.50	0.50	0.0013	1.000	0.444
	0.50	0.20	0.0013	1.000	
	0.50	0.00	0.0013	1.000	
	0.30	0.50	0.0017	1.000	
	0.30	0.20	0.0017	1.000	
	0.30	0.00	0.0017	1.000	
	0.10	0.50	0.0023	1.000	
	0.10	0.20	0.0023	1.000	
	0.10	0.00	0.0023	1.000	
BA	0.50	0.00	0.0013	1.000	0.122
	0.30	0.00	-0.0007	0.000	
	0.10	0.00	-0.0003	0.000	
	0.50	0.20	0.0013	1.000	
	0.30	0.20	-0.0007	0.000	
	0.10	0.20	-0.0003	0.000	
	0.50	0.50	0.0013	1.000	
	0.30	0.50	0.0017	1.000	
	0.10	0.50	-0.0003	0.000	

Table 3: Network structure statistics for ER, WS, and BA models. The adoption rate is an average over all 200 steps. The high adoption probability is based on 30 trial runs and a threshold of 0.9. The Average Clustering Coefficient are the same as they are not affected by initial seeding levels.